

COMBINING IMAGE ANALYSIS AND MODULAR NEURAL NETWORKS FOR AUTOMATIC CLASSIFICATION OF MINERAL INCLUSIONS AND PORES IN ARCHAEOLOGICAL POTTERY: A PILOT STUDY ON SOME SHARDS FROM TAKARKORI ROCK-SHELTER (LYBIAN SAHARA)

ANNA APRILE

Dipartimento di Scienze della Terra e Geoambientali, Università di Bari "Aldo Moro", Via E. Orabona 4, 70125 Bari

ABSTRACT

In this doctorate work, a methodology was developed and assessed by combining image analysis techniques and neural network capabilities to classify some types of mineral inclusions and pores in archaeological potsherds; digital images acquired from thin sections via transmitted-light optical microscopy (plane and cross polarized) were used. Particularly, some Holocene potsherds (9000-3500 years B.P.), belonging to Takarkori rock-shelter archaeological site in the Tadrart Acacus (SW Libya, Central Sahara), were considered as case study to such a purpose. The work may be considered as a pilot study to introduce pattern classification techniques in the field of archaeological ceramic petrography.

The experimentation involved different phases. Image analysis was primarily performed to obtain binary images including regions corresponding to three types of mineral inclusions (*i.e.*, quartz, calcareous aggregates and feldspars) and pores characterizing the considered potsherds. Characteristics observed in both plane and cross polarized images were used to develop a segmentation procedure customized for each type of inclusions and for pores using mathematical operators and automatic thresholding methods. Statistical and region features were finally computed for each segmented region to be used for creation of corresponding neural networks.

Rather than using a monolithic neural network, a modular architecture that combines as many networks (called *modules*) as the number of classes was adopted. Three neural modules were firstly created, each trained to separately recognize quartz, calcareous aggregates and pores, and then combined into the corresponding modular architecture. This architecture was lastly extended introducing a new neural module to classify feldspars via an appropriate incremental strategy. The created modular classifier was then assessed on never-seen-before samples, providing a global classification accuracy of 91.4%. Particularly, the 99.1% of quartz, the 93.6% of calcareous aggregates, the 77.6% of pores and the 95.1% of feldspars were correctly recognized.

The experimentation may be hence considered encouraging for the proposed application. However, further improvements and specific implementations of the methodology should be taken into account in order to better accomplish classification and characterization purposes of ceramic petrography applied to archaeological pottery.

INTRODUCTION

The application of artificial neural networks to image analysis as statistical pattern recognition technique may be considered a growing interesting task in many disciplines involved in digital image processing aimed to object recognition and classification (Jain *et al.*, 2000; Egmont-Petersen *et al.*, 2002). This largely depends on the well-known computational capabilities of neural networks which may be used to solve many pattern classification problems via emulating human learning model and properties such as non-linearity, high parallelism, noise tolerance and generalization (Basheer & Hajmeer, 2000). Generally, a neural network used as pattern classifier learns *features* describing a predetermined number of classes in such a way that, presenting the network successively with an unknown object, it should have the ability to assign the object to one of those previous learned classes. In this procedure, image analysis is used to extract numerical data by the interested objects detected in corresponding digital images to be used as *features* for learning and final classification.

The use of neural networks as image pattern classifiers was recently considered also in optical mineralogy to identify minerals and classify rocks and their textures by digital optical microscope images of thin sections (Thompson *et al.*, 2001; Marmo *et al.*, 2005; Fueten & Mason, 2007; Baykan & Yilmaz, 2010; Singh *et al.*, 2010). Actually, optical microscopy practice generally involves the operator to have sufficient knowledge and experience about optical-based classification and requires various add-ons to the microscope (*e.g.*, special lenses, apertures and filters) to be practicable. Then, neural systems were trained aimed to identify and classify automatically, in a faster and reliable way, rocks and their textures using suitable features about colour, texture and shape of minerals extracted by appropriate processed and segmented digital images of thin sections. For example, optical image processing and artificial neural networks were adopted in the work of Thompson *et al.* (2001) to classify minerals belonging to samples of magmatic, metamorphic and sedimentary rocks. A classification accuracy as high as 93% was here provided. Marmo *et al.* (2005) automatically identify, according to the Dunham classification, carbonate textures unaffected by post-depositional modifications using digital images extracted by more than 1000 thin sections of Phanerozoic carbonates from different marine environments. A set of 23 features were extracted by the images appropriately processed and segmented. An accuracy of 93.4% was finally achieved. Moreover, also Singh *et al.* (2010) proposed the classification of rock texture using neural networks and image analysis. Particularly, RGB or grey-scale image of about 300 thin sections belonging to 140 basalt rock samples were used to extract 27 features. Finally, Baykan & Yilmaz (2010) used 6 features related to colour as extracted by corresponding processed images of selected rock thin sections to classify 5 different minerals, namely quartz, muscovite, biotite, chlorite and opaque.

However, despite of rocks and other derived-manufactured materials, for archaeological materials such as pottery (which can be considered as “artificial rocks” for their mineral-based composition) the application of artificial neural networks as image pattern classifiers has not been yet similarly adopted, yet. Instead, it may believe that neural networks used as image pattern classifiers could have a high potentiality for ancient ceramic investigations. Actually, ability of generalization and learning of neural classifiers may be considered potentially useful to “translate” variability of these heterogeneous materials (which are characterized by highly different fabrics and microstructures) for their classification and description.

To such a purpose, in this PhD thesis pattern classification techniques were introduced in archaeological ceramic petrography. This work may be thus considered as a pilot study in the field.

THE PROPOSED METHODOLOGY

To develop and assess the proposed methodology, some Neolithic potsherds (9000-3500 years B.P.) from Libyan Central Sahara (Eramo *et al.*, in press) were considered as case study.

Particularly, 22 thin sections of these potsherds (belonging to fabrics named QC and QF), characterized by three types of mineral inclusions (namely quartz, calcareous aggregates and feldspars) and secondary porosity, were used (Fig.1).

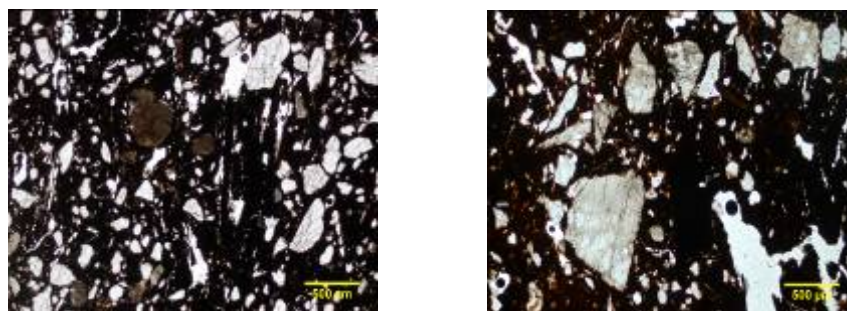


Fig.1 - Fabrics of Takarkori potsherds named QC (left) and QF (right).

Rather than using a single monolithic neural network, which could contemporary classify the four interested classes, a *modular neural architecture* (Auda & Kamel, 1999; Jacobs *et al.*, 1991) was adopted; it was composed by four different neural networks (called *modules*), each trained to separately classify quartz (named *class 1*), calcareous aggregates (named *class 2*), pores (named *class 3*) and feldspars (named *class 4*).

This work involved thus three different phases: *i*) image analysis was performed to isolate regions corresponding to quartz, calcareous aggregates, feldspars and pores in order to extract features for further training of neural modules; *ii*) the modular classifier was created to classify initially only three of the interested classes and *iii*) it was finally extended introducing a new module aimed to classify the fourth class, proving thus scalability of such an architecture.

Image Analysis

Four pairs of RGB digital images each composed by a plane (P) and a cross (XP) polarized light image of 1920×2560 pixel size were acquired, for every thin section, at a magnification of 2.5x using a ZEISS Axioskop 40 Pol petrographic microscope equipped with a Nikon DS-5MC digital camera.

Mathematical operators like addition, subtraction and exponential (Gonzalez & Woods, 2002) were adopted to manipulate both plane and cross polarized light images during image processing in order to emphasize useful characteristics of inclusions and pores. Actually, manipulation of both types of optical images may be particularly suggested because inclusion morphology is generally more clearly defined by observing the plane polarized light images, whereas their mineralogical distinction may be more easily achieved considering the interference colours in cross polarized ones (Whitbread, 1991). In this way, a segmentation procedure was finally developed that was customized for each class to be isolated. The automatic thresholding method *Isodata* (Ridler & Calvard, 1978) was finally applied. A set of 39 statistical and region features (Press *et al.*, 1992; Gonzalez & Woods, 2002; Table 1), referred to the corresponding areas of P and XP images, were computed for each obtained binary region. Particularly, statistical features were computed for each R, G and B colour channel of the images.

The freeware open-source image analysis software ImageJ¹ (version 1.42 and later) was used to perform image processing and its plug-in *Particles8_Plus*² for feature extraction.

Table 1 - Features computed in this work

Statistical	Definition	Region	Definition
Mode	most occurring R-G-B values	Solidity	Area/Convex Area
Median	median R-G-B values	Concavity	Convex Hull-Area
Average	mean R-G-B values	Rectangularity	Area/Area Bounding Box
Variance	mean square deviation of R-G-B values		
Standard Deviation	standard deviation of R-G-B values		
Skewness	degree of asymmetry of R-G-B value distribution		
Kurtosis	peakedness of R-G-B value distribution		
Average Deviation	spread of R-G-B values from average		
Integrated Density	sum of R-G-B values		
Min	minimum R-G-B values		
Max	maximum R-G-B values		
Entropy	degree of variability of R-G-B values		

¹ <http://www.imagej.nih.gov/ij/>

² <http://www.dentistry.bham.ac.uk/landinig/software/software.html>

Creation of the Modular Classifier

Creation of modular classifier was aimed initially to classify three of the classes here considered, namely quartz, calcareous aggregates and pores. To address the neural modules of each class, the *one-vs.-rest* decomposition scheme was used (Chen & You, 1993; Anand *et al.*, 1995); that is, a training set T_c composed by a subset T_c^+ containing the patterns that belong to a class (*positive samples*³) and by a subset T_c^- containing the patterns of the remaining classes (*negative samples*) was created for learning of each class by each module. To such a purpose, the feature-vectors extracted by P and XP images were primarily tested to find the more efficient configuration to be used for each class.

A multilayer perceptron neural network model (MLPNN; Haykin, 1999) was then implemented for each module using the MatLab® NPrTool (Neural Network Pattern Recognition Tool) v.7.10.0 (R2010a). Particularly, a *two-layer* architecture was adopted. A total amount of 16 neural network topologies were trained for each class module, obtained by ranging the hidden neurons from 5 to 80 using a rate of 5 neurons. The network topologies for each class providing the lowest classification error on the test set (*Test Error*), defined as the probability of error in classifying new objects (Wanas *et al.*, 1999), were lastly selected to be used as neural modules.

The modular classifier was finally created by applying the three selected classifiers simultaneously to an *assessment dataset* of unknown patterns (*i.e.*, not considered for training) using the *winner-take-all* strategy (Lu & Ito, 1999) according to which, given an unknown pattern \mathbf{x}^* , the class with the highest confidence value namely $f_c(\mathbf{x}^*) = \max_{k=1...K} f_k(\mathbf{x}^*)$ is the final winning class. Precisely, the modular classifier is said to assign \mathbf{x}^* to class c if the following conditions holds:

$$|f_c(\mathbf{x}^*) - 1| \leq \delta \text{ and } |f_k(\mathbf{x}^*)| < \delta \text{ for } k \neq c \tag{1}$$

where δ is a real number, which denotes the error tolerance (in this work δ is set to 0.5). Let it denote by $f(\mathbf{x})$ the actual output vector of the whole modular classifier, it may be written

$$f(\mathbf{x}) = [f_1(\mathbf{x}), f_2(\mathbf{x}), f_3(\mathbf{x})]^T \tag{2}$$

and thus, for example, $f(\mathbf{x}^*) = [0.9, 0.4, 0.1]$ means that pattern \mathbf{x}^* belongs to class 1, $f(\mathbf{x}^*) = [0.3, 0.7, 0.2]$ means that pattern \mathbf{x}^* belongs to class 2 and $f(\mathbf{x}^*) = [0.3, 0.3, 0.8]$ means that pattern \mathbf{x}^* belongs to class 3 (Fig. 2).

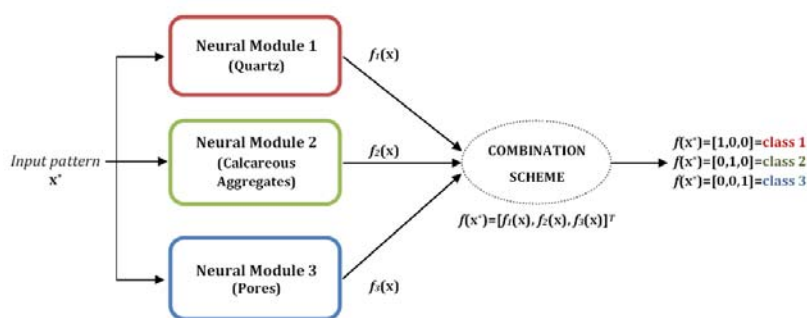


Fig. 2 - Schematic representation of the created modular classifier.

³ The term *sample* or pattern indicates each segmented region of the interested classes with its corresponding feature-vector.

Extension of the Modular Classifier

A new neural module, aimed to classification of feldspars (class 4), was then introduced to extend the modular architecture. Seven training datasets were arranged here, which derived by all possible combinations of the interested class samples according to the *one-vs.-rest* decomposition scheme. The same conditions for training were adopted and, similarly, the classification error on the test was finally considered.

Next, an incremental strategy was provided to integrate the new classifier into the pre-existing modular architecture. To such a purpose, a neural network denoted as *combiner* was trained which used as input features also the *answers* (i.e., the outputs) obtained by each of the four modules, performing thus a *tuning operation*. Actually, the output of the combiner was a four-weight vector w (having values ranging from 0 to 1), which returned a weighted final output for the extended modular neural classifier taking into account a balanced contribution of each class to the overall classification performance (Fig. 3). A total amount of 8 neural networks topologies were trained by considering a number of hidden neurons ranging from 10 to 80 and by using a rate of 10 neurons to select the optimal topology for the combiner.

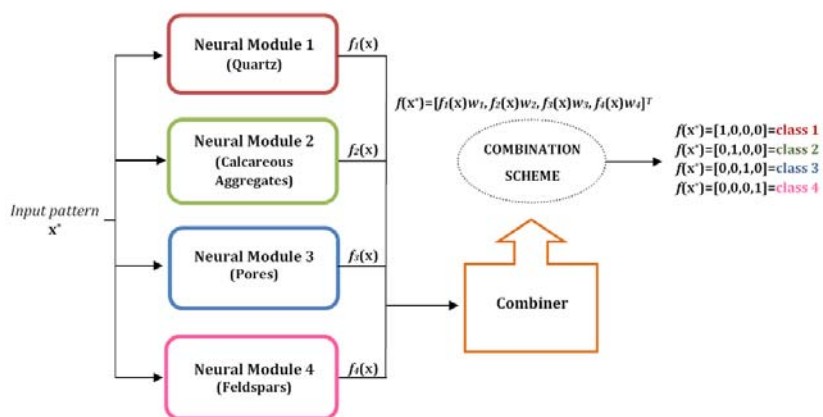


Fig. 3 - Schematic representation of the adopted incremental strategy.

The experimentation was finally concluded by creating a three-class and a four-class monolithic classifier to contemporary distinguish among the considered classes to be compared with corresponding modular and extended modular classifier.

RESULTS

Binary images containing 41085 regions corresponding to quartz, 9313 to calcareous aggregates, 35258 to pores and 2594 to feldspars, for a total of 88250 regions, were finally obtained (Fig. 4) and corresponding 39-feature vectors were derived both by P and XP images.

The preliminary test performed to select the features to be used for each class training set returned the better accuracy for features extracted by XP images for both quartz and calcareous aggregates and by P images for both pores and feldspars.

The number of positive samples (T^+) in the training sets belonging to each class was finally established by considering the number of available samples for the less abundant class (i.e., class of feldspars). Particularly, 1200 samples for each class were selected to such a purpose. Moreover, an equal number of samples corresponding on the whole to the number of positive samples was considered for the remaining classes to be used as negative samples (T).

The $39 \times 25 \times 1$, the $39 \times 5 \times 1$ and again the $39 \times 5 \times 1$ topologies were finally selected as neural modules for quartz, calcareous aggregates and pores, respectively with a training accuracy (Test Error) of 97.6%, 99.4% and 100%. Moreover, the $39 \times 15 \times 1$ and the $43 \times 10 \times 1$ topologies were selected respectively as module of feldspars and as combiner with a training accuracy of 74.8% and 97.5%.

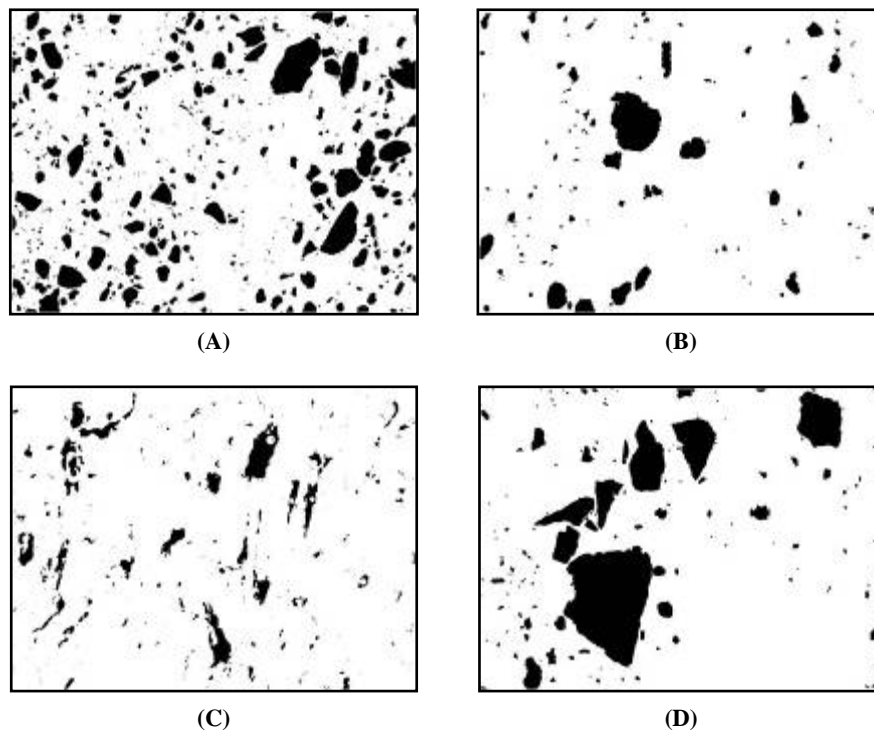


Fig. 4 - Example of binary regions of quartz (A), calcareous aggregates (B), pores (C) and feldspars (D).

Among the remaining samples available for each class, a total of 3000 were used to create the *assessment dataset* (namely 1000 unknown samples for each of the three considered classes) and hence to assess the modular classifier. Next, the assessment dataset was grown by adding also 1000 unknown samples of feldspars to assess also the extended modular classifier.

Classification accuracy of modular and extended modular classifier are reported in the corresponding confusion matrices (Fig. 5). Particularly, the modular classifier globally provided a classification accuracy of 89.8% on the assessment dataset, which was particularly higher for calcareous aggregates and quartz (99.1% and 93.6% respectively), whereas it was lower for the class of pores (76.6%). Moreover, the quartz was mainly confused with the calcareous aggregates (58 errors over 64), the calcareous aggregates with the pores (6 errors over 9) and finally the pores were confused largely with the quartz (178 errors over 234).

On the other hand, the extended modular classifier accuracy was higher mainly for quartz (99.0%) and also for feldspars (95.1%) and calcareous aggregates (93.6%) respectively, whereas it was lower for class of pores (77.6%). Quartz was confused here with calcareous aggregates (10 errors over 10), calcareous aggregates with feldspars (59 errors over 61) and vice versa (36 errors over 49). Finally, pores were confused mainly with quartz (162 errors over 224). A classification accuracy of 91.4% was globally returned by the extended modular classifier.

Finally, the $39 \times 10 \times 3$ and the $39 \times 50 \times 4$ topologies were selected as corresponding three-class and four-class trained monolithic classifier. Particularly, the classification accuracy finally provided on the same assessment dataset was higher for the three-class monolithic classifier than for the four-class (88.7% and 83.8%, respectively).

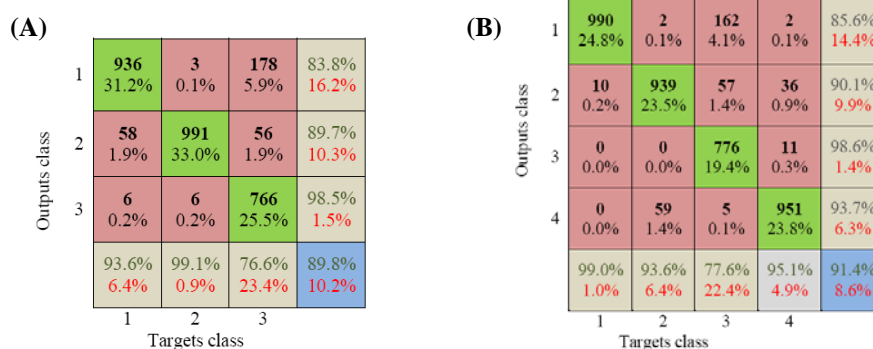


Fig. 5 - Confusion matrix of the modular (A) and of the extended modular classifier (B).

DISCUSSION

Segmentation was provided here thanks to the combined use of mathematical operators coupled with an automatic thresholding method. The effectiveness of this segmentation procedure was just proved by Eramo *et al.* (in press) since it was observed to be appropriate for all the samples investigated, which were easily and uniformly segmented in this way.

Differently as expected due to their well-known optical similarity (Edwards, 2008), quartz and feldspars were not confused one with each other and rather recorded the higher classification accuracy. Especially, image acquisition strategy adopted for feldspars (namely images were captured in twinning positions) was thus proved to be powerful. Actually, feldspars and quartz show similar RGB values both in plane polarized and in cross polarized images but image texture provided by twinning allowed to distinguish feldspars by quartz, particularly in plane polarized images. Statistical features describing texture like *Entropy* (for each RGB channel) both with region features informing on shape like *Solidity* and *Rectangularity* were proved particularly to have a more discriminating ability to such a purpose.

Oppositely, a lower classification accuracy was achieved for class of pores. Particularly, pores were observed to be mainly confused with quartz. Such misclassification was proved to be related to some samples of pores localized in plane polarized image, which had similar RGB values as the quartz in plane polarized images, recalling that features of both kind of images were respectively used for creation of corresponding neural modules. Moreover, most of the statistical features for pores and quartz were observed to show similar values, namely to have low discriminating ability in this case.

Globally, it was especially observed that region features named *Solidity* and *Rectangularity* both with statistical ones named *Entropy*, *Skewness* and *Kurtosis* influenced classification accuracy improvement.

Moreover, it must be noticed that classification accuracy globally increased after extending the created modular classifier. Actually, the incremental approach performed by the *combiner* let the modular classifier model developed to be flexible and thus easy-to-extend.

Finally, both for modular and extended modular classifier, a lower classification accuracy was provided here by corresponding monolithic networks. It was then verified that, if the monolithic structure is grown, global classification accuracy decreases and time needed for training increases, as reported by the literature (Auda & Kamel, 1999).

CONCLUSIONS

The results obtained in this experimentation may be considered encouraging. Due to the lack of application in archaeometry of such an approach, which combines image analysis and particularly modular neural networks, it might be difficult to compare these results as well as advantages and problems encountered

throughout this experimentation. However, the advantages of modular neural architecture implementation was proved here as just for other pattern recognition problems (Auda & Kamel, 1999). These would be considered particularly promising for more complex archaeological pottery fabrics, including a large number of mineral inclusions (*e.g.*, micas, amphiboles or pyroxenes) as well as for different kind of porosity. Actually, only incremental strategy needs to be controlled and, if ever necessary, appropriately improved, as well as new modules will be added.

However, further improvements and implementation of the methodology may be considered in order to better accomplish classification and characterization purposes aimed by ceramic petrography. For example, future work for the case here proposed may be devoted primarily to search for an optimization of feature selection, as seen for class of pores. Moreover, the created modular classifier may be practically applied for classification of these types of inclusions and pores of different archaeological potsherds.

REFERENCES

- Anand, R., Mehrotra, K.G., Mohan, C.K., Ranka, S. (1995): Efficient classification for multiclass problems using modular neural networks. *IEEE T. Neural Networ.*, **6**, 117-124.
- Auda, G. & Kamel, M. (1999): Modular neural networks: a survey. *Int. J. Neural Syst.*, **9**, 129-151.
- Basheer, I.A & Hajmeer, M. (2000): Artificial neural networks: fundamentals, computing, design, and application. *J. Microbiol. Meth.*, **43**, 1, 3-31.
- Baykan, N.A. & Yilmaz, N. (2010): Mineral identification using color spaces and artificial neural networks. *Comput. Geosci.*, **36**, 91-97.
- Chen, C.H. & You, G.H. (1993): Class-sensitive neural network. *Neural Parallel Sci. Comput.*, **1**, 93-96.
- Edwards, M.G. (2008): Introduction to optical mineralogy and petrography: the practical methods of identifying minerals in thin section with the microscope and the principles involved in the classification of rocks. Camp Press, Cleveland, Ohio. 208 p.
- Egmont-Petersen, M., de Ridder, D., Handels, H. (2002): Image processing with neural networks-a review. *Pattern Recogn.*, **35**, 2279-2301.
- Eramo, G., Aprile, A., Muntoni, I.M., Zerboni, A. (in press): Textural and morphometric analysis applied to Holocene pottery from Takarkori rock shelter (SW Libya, Central Sahara): a quantitative sedimentological approach. *Archaeometry*, DOI: 10.1111/arc.12043.
- Fueten, F. & Mason, J. (2007): An artificial neural net assisted approach to editing edges in petrographic images collected with the rotating polarizer stage. *Comput. Geosci.*, **33**, 1176-1188.
- Gonzalez, R.C. & Woods, R.E. (2002): Digital image processing. Prentice Hall, Inc., Upper Saddle River, New Jersey. 793 p.
- Haykin, S. (1999): Neural Networks: a Comprehensive Foundation. Macmillan, New York, 823 p.
- Jacobs, R.A., Jordan, M.I., Barto, A.G. (1991): Task decomposition through competition in a modular connectionist architecture: the what and where vision tasks. *Cognitive Sci.*, **15**, 219-250.
- Jain, A.K., Duin, R.P.W., Mao, J. (2000): Statistical pattern recognition: a review. *IEEE T. Pattern. Anal.*, **22**, 1, 4-37.
- Lu, B.-L. & Ito, M. (1999): Task decomposition and module combination based on class relations: a modular neural network for pattern classification. *IEEE T. Neural Networ.*, **10**, 1244-1256.
- Marmo, R., Amodio, S., Tagliaferri, R., Ferreri, V., Longo, G. (2005): Textural identification of carbonate rocks by image processing and neural network: Methodology proposal and examples. *Comput. Geosci.*, **31**, 649-659.
- Press, W.H., Teukolsky, S.A., Vetterling, W.T., Flannery, B.P. (1992): Numerical Recipes in C, The Art of Scientific Computing. Cambridge University Press, Cambridge, UK, 610 p.
- Ridler, T.W. & Calvard, S. (1978): Picture thresholding using an iterative selection method. *IEEE T. Syst, Man Cyb.*, **8**, 630-632.
- Singh, N., Singh, T.N., Tiwary, A., Sarkar, K.M. (2010): Textural identification of basaltic rock mass using image processing and neural network. *Comput. Geosci.*, **14**, 301-310.
- Thompson, S., Fueten, F., Bockus, D. (2001): Mineral identification using artificial neural networks and the rotating polarizer stage. *Comput. Geosci.*, **27**, 1081-1089.
- Wanas, N., Kamel, M.S., Auda, G., Karray, F. (1999): Feature-based decision aggregation in modular neural network classifiers. *Pattern Recogn. Lett.*, **20**, 1353-1359.
- Whitbread, I.K. (1991): Image and data processing in ceramic petrology. In: "Recent Developments in Ceramic petrology", A. Middleton & I.C. Freestone, eds. British Museum Publications Ltd., London, 369-388.